Mathematical Biosciences 355 (2023) 108936

Contents lists available at ScienceDirect

Mathematical Biosciences

journal homepage: www.elsevier.com/locate/mbs

Original Research Article

The impact of temperature and decay in insecticide-treated net efficacy on malaria prevalence and control

Calistus N. Ngonghala *

Department of Mathematics, University of Florida, Gainesville, FL 32611, USA
Emerging Pathogens Institute, University of Florida, Gainesville, FL 32610, USA
Center for African Studies, University of Florida, Gainesville, FL 32611, USA

ARTICLE INFO

Keywords:
Malaria transmission and control
Mosquito-borne disease model
Waning insecticide-treated net efficacy
Temperature change and seasonality
Reproduction number
Sensitivity analysis

ABSTRACT

Insecticide-treated nets (ITNs) have been useful and effective in mitigating the risk of malaria globally. However, due to misuse and normal/human-induced physical and chemical wear, the effectiveness of ITNs in combating malaria has been declining. Underlying heterogeneities in the nature of malaria, combined with environmental factors such as temperature lead to complex malaria transmission and control dynamics. In particular, temperature plays a significant role in determining the risk of malaria since it influences the growth and survival of mosquitoes and the malaria parasite. Here, a unifying mechanistic framework that integrates malaria dynamics with waning ITN-efficacy and temperature change is developed and used to assess the impact of interactions between significant sources of variation (e.g., temperature) and waning ITN-efficacy on the risk of malaria transmission and the success of ITN programs. The model exhibits a backward bifurcation when ITN-efficacy is constant implying that control efforts must be stepped up and sustained a bit longer even when the reproduction number is slightly less than one. The study shows that malaria is more effectively controlled with ITNs that have a longer lifespan and if ITNs are replaced before the end of their expiration period. Also, failing to account for waning ITN-efficacy leads to an underestimation of disease risk, burden, and effort level required to contain the disease. Local and global sensitivity analyses show that control and temperature-related parameters are primary drivers of the reproduction number and the human disease burden, highlighting the significance of temperature on malaria dynamics. Furthermore, the study shows that the human disease burden is optimal at a temperature of ≈28°C and that high seasonal variations can trigger major malaria outbreaks even in regions with low mean temperatures. Additionally, accounting for both seasonality and decay in ITN-efficacy leads to complex malaria patterns. To sum it up, insights into the sensitivity of malaria dynamics on temperature are useful in assessing the potential impact of changes in temperature on malaria risk. Also, a malaria control program, which ensures that ITNs are replaced regularly and early enough, and that educates at risk populations on proper use and care for ITNs is necessary for reducing the burden of malaria.

1. Introduction

Human health is challenged by infectious diseases on a global scale. These infectious diseases include vector-borne diseases such as malaria, Zika virus, Dengue fever, etc., whose transmission from one human to another is facilitated by mosquitoes. The main association between humans, mosquitoes, and the causative agents (e.g., parasites and viruses) of vector-borne diseases are blood meals required by female mosquitoes for reproduction. The female *Anopheles* mosquito has been implicated for its contribution in the transmission of one of the oldest, most prevalent, and life-threatening micro-parasitic human vector-borne diseases (malaria). Because of its established role in spreading the protozoan, *Plasmodium falciparum* — the deadliest form of the human malaria parasite in sub-Saharan Africa [1], the *Anopheles gambiae* complex is one of the well-known species of *Anopheles* mosquitoes. Underlying heterogeneities in the transmission of malaria (e.g., the life cycle of the malaria parasite is shared between humans and *Anopheles* mosquitoes) coupled with environmental factors such as changes in temperature, humidity, and precipitation affect the transmission dynamics of malaria and the success of malaria control and mitigation programs.

Despite the significant decline in the number of malaria cases and deaths around the world within the past two decades, malaria continues to be a leading cause of morbidity, mortality, and economic hardship in many regions of the world [2–4], especially in sub-Saharan Africa, which harbored about 95% of the global malaria cases in 2020 [5]. Specifically, approximately 241 million confirmed clinically cases of malaria and 627,000 malaria-related deaths were reported globally in

* Correspondence to: Department of Mathematics, University of Florida, Gainesville, FL 32611, USA.
E-mail address: calistusnn@ufl.edu.

https://doi.org/10.1016/j.mbs.2022.108936
Received 12 July 2022; Received in revised form 28 October 2022; Accepted 31 October 2022
Available online 7 November 2022

2020 [5]. This represented a 6.2% (12%) increase in the number of clinical malaria cases (malaria-related deaths) in comparison to the number of cases (deaths) reported in 2019 [6]. More than half of the additional malaria-induced deaths in 2020 were caused by disruptions in malaria control programs during the COVID-19 pandemic [5].

A variety of control and mitigation measures against malaria transmission are available. These include artemisinin-based combination therapy, intermittent preventive treatment and vector intervention strategies such as eliminating mosquito habitats near human dwellings, indoor residual spraying, and insecticide-treated nets (ITNs), [7–13]. Sustained vector control has been shown to work well in malaria control and efforts directed toward malaria elimination [14–16]. One of the most effective and core vector control measures (ITN-use) has been critical in interrupting the malaria transmission cycle by preventing contacts between humans and crepuscular, nocturnal, or endophagic mosquitoes (i.e., mosquitoes that are active at dawn or dusk, night, or indoors) such as some species of *Anopheles* mosquitoes. As a result of ITN-use, the number of malaria cases has been reduced globally by approximately 68% since 2000 [17]. While ITNs have been widely adopted as the major malaria control and mitigation measure in many malaria-endemic regions around the world, their success is undermined by waning of the efficacy of ITNs due to natural and chemical deterioration resulting from improper handling and usage, lengthy exposure to intense sunshine, frequent washing, and using ITNs for purposes other than protection [18–23]. For example, although over 65% of the populace of sub-Saharan Africa owned at least one ITN in 2020, only 43% of this populace used ITNs for protection against mosquito bites.

The transmission intensity of malaria is determined by a number of factors that are associated with the malaria parasite, vector, the human host, and the environment. In particular, the malaria vector and parasite are sensitive to environmental conditions such as temperature, humidity, rainfall, etc. Several studies have shown that temperature is an important driver of malaria risk since it influences both the *Anopheles* mosquito and *Plasmodium* parasite growth and survival rates, as well as the biting rate of mosquitoes [24–34]. Some mosquitoes prefer warm and humid climates, while low or high temperatures can cause mosquitoes to be less active. Some mosquitoes hibernate at low temperatures and excessive heat can dehydrate mosquitoes [25–27]. Malaria transmission is seasonal in many regions, with a possible surge during and immediately following the wet season. Furthermore, malaria epidemics can emerge in populations with low or nonexistent immunity to malaria when environmental conditions and other factors favor malaria transmission. Hence, recent gains in global malaria control are threatened by current increasing temperature and variable weather patterns.

Although independent mathematical models have been developed and used to study the impact of ITNs and decay in ITN-efficacy [13,35–42], as well as the impact of temperature and seasonal variation [27,29,30,34,43–46] on malaria risk and control, there is no unifying framework that assesses the combined impact of decay in ITN efficacy and temperature/seasonal fluctuations on malaria transmission risk and dynamics. The goal of this project is to bridge this gap by developing a mechanistic framework that integrates malaria dynamics with decaying in ITN efficacy, temperature change, and seasonal variation and using the framework to investigate how significant sources of variation (e.g., temperature change) interact with waning ITN-efficacy to impact the risk of malaria transmission and the success of ITN programs.

2. Methods and materials

2.1. The model with decaying ITN-efficacy

The model system that we study here is constructed by dividing the total human population (denoted by N_h) into susceptible (S_h), exposed or incubating (E_h), infectious (I_h), and recovered (R_h) individuals. Similarly, the total mosquito population (denoted by N_v) is split into susceptible (S_v), exposed or incubating (E_v), and infectious (I_v) mosquitoes. Since there is no empirical evidence that mosquitoes recover from malaria infection, we ignore the recovered class for mosquitoes. The recovered class (for humans) consists of humans with incomplete immunity, who can also transmit the infection to other humans via mosquitoes. Since malaria does not confer permanent immunity, partially immune individuals can lose their immunity and become susceptible to the disease again. It is assumed that all births in both the human and the mosquito populations are into the susceptible classes, i.e., there is no vertical transmission of malaria.

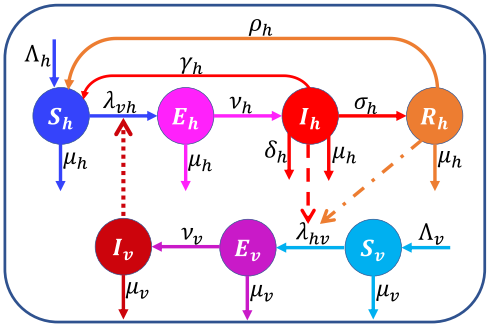

Fig. 1. Schematic illustration of the malaria model. The model has four human classes: susceptible (S_h), exposed or incubating (E_h), infectious (I_h), and recovered (R_h), and three mosquito classes: susceptible (S_v), exposed or incubating (E_v), and infectious (I_v). Flow of individuals between classes is represented by solid lines. Malaria transmission from the infectious (partially immune) human class is denoted by a dashed (dashed–dotted) line, while transmission from the infectious mosquito class to the susceptible human class is denoted by a dotted line. The model parameters are described in Table 1.

Schematics and brief explanations of the parameters of the model are presented in Fig. 1 and Table 1, respectively. Following the Schematics (in Fig. 1), descriptions of the model variables, and the tabular description of the model parameters (Table 1), the human and mosquito population dynamics, as well as the transmission dynamics of malaria between these two populations are characterized by the model system:

$$\begin{aligned}
\dot{S}_h &= \Lambda_h + \gamma_h I_h + \rho_h R_h - (\lambda_{vh} + \mu_h) S_h,\\
\dot{E}_h &= \lambda_{vh} S_h - (\mu_h + \nu_h) E_h,\\
\dot{I}_h &= \nu_h E_h - (\delta_h + \gamma_h + \mu_h + \sigma_h) I_h,\\
\dot{R}_h &= \sigma_h I_h - (\mu_h + \rho_h) R_h,\\
\dot{S}_v &= f_v(N_v, \theta) N_v - [\lambda_{hv}(\theta) + \mu_v(\theta)] S_v,\\
\dot{E}_v &= \lambda_{hv}(\theta) S_v - [\mu_v(\theta) + \nu_v(\theta)] E_v,\\
\dot{I}_v &= \nu_v(\theta) E_v - \mu_v(\theta) I_v,
\end{aligned} \tag{2.1}$$

where θ is temperature in degrees Celsius (°C). The dynamics of the total human and mosquito populations are described by the equations

$$\dot{N}_h = \Lambda_h - \mu_h N_h - \delta_h I_h, \qquad \dot{N}_v = [f_v(N_v, \theta) - \mu_v(\theta)] N_v. \tag{2.2}$$

As in Ngonghala et al. [45,47], the mosquito birth rate is modeled through the logistic growth functional form:

$$f_v(N_v, \theta) = \alpha_v(\theta)\left(1 - \frac{N_v}{\kappa_v}\right), \quad \alpha_v(\theta) = \xi_e(\theta) p_e(\theta) \phi_e(\theta) \mu_v(\theta)^{-1}, \tag{2.3}$$

where ξ_e is the number of eggs per female mosquito per day, p_e is the survival probability from egg to adult mosquito, ϕ_e is the development rate from eggs to the adult mosquito stage (i.e., $1/\phi_e$ is the average egg to adult development time), and κ_v is the mosquito carrying capacity (i.e., the amount of resource available for mosquito sustenance). Following Ngonghala et al. [39–41], the mosquito to human (human to mosquito) force of infection λ_{vh} (λ_{hv}) are modeled by the functions

$$\lambda_{vh}(b_\beta, \theta) = \frac{p_{vh} \beta(t, \theta) I_v}{N_h}, \text{ and } \lambda_{hv}(b_\beta, \theta) = \frac{p_{hv}(\theta) \beta(t, \theta)(I_h + \epsilon_r R_h)}{N_h}, \tag{2.4}$$

Table 1
Brief descriptions of parameters of the model system (2.1) and biologically feasible values and ranges for the parameters.

Parameter	Description	Unit	Baseline value	Range	Reference
Λ_h	Human recruitment rate	Humans per day	$10^3/(61\times 365)$	$[10^3/75, 10^3/53]\times 1/365$	[49]
$1/\nu_h$	Human latent period	Day	14	$[10/2, 10^3/67]$	[50–52]
$1/\rho_h$	Duration of human immunity	Day	5×365	$[10^3/11, 10^6/55]$	[52]
$1/\gamma_h$	Duration of human infection	Day	60	[4, 180]	[53]
$1/\sigma_h$	Duration of human infection	Day	285	$[10^3/17, 10^4/14]$	[52]
δ_h	Human disease death rate	Per day	$32.9/(365\times 10^3)$	$[0, 41/10^5]$	[52]
$1/\mu_h$	Human life span	Day	61×365	$[53, 75]\times 365$	[49]
p_{vh}	Infectivity of infectious mosquito	Unitless	$22/1000$	$[1/10^2, 27/10^2]$	[52,54–56]
p_{hv}	Infectivity of infectious humans	Unitless	$48/100$	$[72/10^3, 64/10^2]$	[52,57–59]
$\epsilon_r p_{hv}$	Infectivity of immune humans	Unitless	$48/10^3$	$[72/10^4, 64/10^2]$	[52,57–59]
β_u	Maximum mosquito biting rate	Per day	5/10	[1/10,1]	[52,60,61]
β_l	Minimum mosquito biting rate	Per day	1/100	[0,1/10]	Assumed
b_0	ITN coverage	Unitless	$43/100$	$[40/100, 80/100]$	[4]
ϵ_0	Initial ITN efficacy	Unitless	0.9	[0, 1]	Assumed
T	Useful ITN lifespan	Day	3×365	$[180, 3\times 365]$	[62–64]
ξ_e	Eggs laid per female mosquito	Per day	18.8	[13.08, 23.14]	[65]
p_e	Egg to adult survival probability	Unitless	0.58425	[0.273, 0.787]	[25]
$1/\phi_e$	Egg to adult development time	Day	16.3883	[10, 23.302]	[25]
κ_v	Carrying capacity	Mosquitoes	10^4	$[10^3, 5\times 10^4]$	Assumed
$1/\nu_v$	Extrinsic incubation period	Day	13	$[10^2/33, 10^3/29]$	[52,66]
$1/\mu_{v0}$	Mosquito lifespan	Day	14	[7, 21]	[54,67]
μ_{v1}	ITN mosquito mortality rate	Per day	1/14	[1/21, 1/7]	[68]
n	Shape constant	Unitless	6	variable	[39,40]

where $\beta(t,\theta) = \beta_u(\theta) - [\beta_u(\theta) - \beta_l(\theta)]\epsilon_\beta(t)b_0$, with

$$\epsilon_\beta(t) = \frac{2^n+1}{2^{n+1}}\left[\frac{2^n-1}{2^n+1} + \frac{1}{1+\left(\frac{t \bmod T}{T/2}\right)^n}\right]\epsilon_0. \tag{2.5}$$

Furthermore, as in Ngonghala et al. [39–41], the mosquito mortality rate (μ_v) is given by $\mu_v(t,\theta) = \mu_{v0}(\theta) + \mu_{v1}(\theta)\epsilon_{\mu_v}(t)b_0$, where

$$\epsilon_{\mu_v}(t) = \frac{2^n+1}{2^n}\left[-\frac{1}{2^n+1} + \frac{1}{1+\left(\frac{t \bmod T}{T/2}\right)^n}\right]\epsilon_0. \tag{2.6}$$

Here, $0 \le b_0 \le 1$ is the community ITN coverage (i.e., the proportion of the population that uses ITNs), $0 \le \epsilon_0 \le 1$ is the initial (protective and killing) efficacy of ITNs and T is the effective useful lifespan of ITNs. The ITN efficacy for protecting humans from mosquito bites given by Eq. (2.5), and for killing mosquitoes that land on ITNs given by Eq. (2.6) are designed to account for the fact that once insecticide in a net is lost, the initial efficacy of the ITN is reduced by approximately half [48]. Also, since ITNs become less effective over the course of their useful lives (because their efficacy decline with time) as a result of several factors that include misuse and physical/chemical wear, the ITN efficacy functions (2.5)–(2.6) are decreasing functions of time. Furthermore, the functions account for the fact ITNs are replaced following the expiration of their effective useful lives. It should be noted that other functions, such as exponential decay and modified Hill or Weibull functions can also be used.

2.2. Introducing temperature and seasonality

Some of the mosquito-related parameters of the model (2.1), e.g., the egg-to-adult mosquito development rate (ϕ_e), the mosquito biting rate (β), the mosquito (extrinsic) incubation period ($1/\nu_v$), the number of eggs per female adult mosquito per day (ξ_e), the survival probability of eggs (p_e), and the natural mortality rate of mosquitoes (μ_{v0}), depend on temperature and other environmental and climatic conditions [34,47,69]. Two types of functional forms have been used to model the temperature dependent parameters. In particular, the Brière function, $c\theta(\theta-\theta_{min})(\theta_{max}-\theta)^{1/2}$ [70],where c is a modified rate constant, while θ_{min} and θ_{max} denote (critical) minimum and maximum temperatures, has been used to model ϕ_e, β, and ν_v [25,34,71], while the quadratic functional form, $q\theta^2 + r\theta + s$, where q, r, and s are fit parameters has been used to model ξ_e, p_e, and μ_{v0} [25,34,65,72]. See [34,47] for illustrations of some temperature response functions and [34,73–75] for justifications of the unimodal shape of the temperature response functions. The parameter values associated with the temperature-dependent functional forms are presented in Table 2.

On the other hand, the function

$$\theta(t) = \theta_m + \theta_a \sin\left(\frac{2\pi}{365}\right)t, \tag{2.7}$$

where θ_m and θ_a represent the average yearly temperature and the amplitude of the yearly temperature fluctuations, respectively, is used to incorporate seasonal variation into the malaria model (2.1).

3. Results

3.1. Analytical results for the special case in which ITN-efficacy is constant and temperature is not considered

When ITN efficacy is constant (i.e., $\epsilon_\beta = \epsilon_{\mu_v} = \epsilon_0$), and each of the temperature-dependent parameters (i.e., ϕ_e, ξ_e, p_e, β, ν_v, and μ_{v0}) are constant, Eqs. (2.1) can have three possible types of equilibrium points — a mosquito-free equilibrium (E_{mf}), which depicts a situation in which there are no mosquitoes in the community; a disease-free equilibrium (E_{df}), which represents a situation in which there is no malaria in the population; and an endemic equilibrium (E_e), which represents a situation in which the disease is always present at certain levels in the population. These equilibria are obtained by setting $\epsilon_\beta = \epsilon_{\mu_v} = \epsilon_0$ in Eqs. (2.1), setting the left hand sides of the modified model to zero, and solving the system of algebraic equations for the variables.

3.1.1. Disease-free equilibria, and the reproduction number

The model (2.1) with constant ITN efficacy has a mosquito-free equilibrium $E_{mf} = \left(\frac{\Lambda_h}{\mu_h}, 0, 0, 0, 0, 0, 0\right)$ and a disease-free equilibrium $E_{df} = \left(\frac{\Lambda_h}{\mu_h}, 0, 0, 0, \frac{\kappa_v\mu_v}{\alpha_v}(\mathcal{R}_m - 1), 0, 0\right)$, where $\mathcal{R}_m = \frac{\alpha_v}{\mu_v}$. It should be mentioned that the disease-free equilibrium (E_{df}) exists when $\mathcal{R}_m > 1$ (i.e., if $\alpha_v - \mu_v > 0$). When $\mathcal{R}_m \le 1$, only the mosquito-free equilibrium (E_{mf}) exists. The threshold quantity $\mathcal{R}_m$ is called the vectorial reproduction number; it is defined as the average number of new mosquitoes produced by a single female mosquito in an area where there are no mosquitoes through out the lifespan of the female mosquito [39,40].

The next generation matrix approach [77,78] and the disease-free equilibrium (E_{df}) are used to compute the reproduction number

Table 2
Temperature-dependent parameters, their functional forms, and baseline values for additional parameters in the functional forms. Two types of functional forms have been used to model the temperature dependent parameters: The Brière function $(c\theta(\theta-\theta_{min})(\theta_{max}-\theta)^{1/2})$ [70] and the quadratic functional form $(q\theta^2+r\theta+s)$. Here, θ denotes temperature in degrees Celsius, c is a modified rate constant, while θ_{min} and θ_{max} denote (critical) minimum and maximum temperatures, and q, r, and s and fit parameters.

Trait	Brief description and unit	Brière function			Source
		c	θ_{min}	θ_{max}	
ϕ_e	Egg-to-adult development rate (day^{-1})	1.11×10^{-4}	14.7	34.0	[25,34]
β_u	Maximum mosquito biting rate (day^{-1})	2.03×10^{-4}	11.7	42.3	[34,76]
ν_v	1/(extrinsic incubation period) (day^{-1})	1.11×10^{-4}	14.7	34.4	[34,71]
Trait	Brief description and unit	Quadratic function			Source
		q	r	s	
ξ_e	Eggs laid by a female mosquito (day^{-1})	-1.53×10^{-1}	8.61×10^{0}	-9.77×10^{1}	[34,65]
p_e	Survival probability of eggs (no unit)	-0.92×10^{-2}	4.53×10^{-1}	-4.77×10^{0}	[25,34]
μ_{v0}	Natural mosquito mortality rate (day^{-1})	-8.28×10^{-4}	3.67×10^{-2}	5.22×10^{-1}	[34,72]

(i.e., the spectral radius of the matrix, $\mathscr{F}\mathscr{V}^{-1}$) of the model (2.1). Since

$$\mathscr{F}=\begin{pmatrix} 0 & 0 & 0 & 0 & p_{vh}\beta \\ 0 & 0 & 0 & 0 & 0 \\ 0 & 0 & 0 & 0 & 0 \\ 0 & \frac{\beta p_{hv}\mu_h\mu_v\kappa_v(\mathscr{R}_m-1)}{\alpha_v\Lambda_h} & \frac{\beta p_{hv}\epsilon_r\mu_h\mu_v\kappa_v(\mathscr{R}_m-1)}{\alpha_v\Lambda_h} & 0 & 0 \\ 0 & 0 & 0 & 0 & 0 \end{pmatrix} \text{ and}$$

$$\mathscr{V}=\begin{pmatrix} A_1 & 0 & 0 & 0 & 0 \\ -\nu_h & A_2 & 0 & 0 & 0 \\ 0 & -\sigma_h & A_3 & 0 & 0 \\ 0 & 0 & 0 & A_4 & 0 \\ 0 & 0 & 0 & -\nu_v & \mu_v \end{pmatrix},$$

$$\mathscr{F}\mathscr{V}^{-1}=\begin{pmatrix} 0 & 0 & 0 & \frac{p_{vh}\beta\nu_v}{\mu_v A_4} & \frac{p_{vh}\beta}{\mu_v} \\ 0 & 0 & 0 & 0 & 0 \\ 0 & 0 & 0 & 0 & 0 \\ \frac{\beta p_{hv}\nu_h\mu_v A_0}{\alpha_v\Lambda_h A_1 A_2 A_3} & \frac{\beta p_{hv}\mu_v A_0}{\alpha_v\Lambda_h A_2 A_3} & \frac{\beta p_{hv}\epsilon_r\mu_h\mu_v\kappa_v(\mathscr{R}_m-1)}{\alpha_v\Lambda_h A_3} & 0 & 0 \\ 0 & 0 & 0 & 0 & 0 \end{pmatrix}$$

and the reproduction number is given by

$$R_c=\sqrt{\frac{\beta^2 p_{hv}p_{vh}\nu_h\nu_v A_0}{\alpha_v\Lambda_h A_1 A_2 A_3 A_4}}, \tag{3.1}$$

where $A_0=(A_3+\epsilon_r\sigma_h)\mu_h\kappa_v(\mathscr{R}_m-1)$, $A_1=\mu_h+\nu_h$, $A_2=\delta_h+\gamma_h+\mu_h+\sigma_h$, $A_3=\mu_h+\rho_h$, and $A_4=\mu_v+\nu_v$.

The control reproduction number (R_c) is a threshold quantity that can be used to determine whether a disease can be contained (when it is less than one) or will establish itself (when it is greater than one) in a population. Here, R_c represents the expected number of new malaria cases caused by an infected individual during the infectious period of this individual in a population in which some people are protected by ITNs. It should be mentioned that R_c becomes the basic reproduction number (R_0) when no malaria control strategies are utilized. The reproduction numbers $\mathscr{R}_m$ and R_c will now be used to establish the stability of the mosquito-free and disease-free equilibria.

3.1.2. Local and global stability of the mosquito-free equilibrium

The Jacobian of the system at the mosquito-free equilibrium is

$$J_{mf}=\begin{pmatrix} -\mu_h & 0 & \gamma_h & \rho_h & 0 & 0 & -\beta_v p_{vh} \\ 0 & -A_1 & 0 & 0 & 0 & 0 & \beta_v p_{vh} \\ 0 & \nu_h & -A_2 & 0 & 0 & 0 & 0 \\ 0 & 0 & \sigma_h & -A_3 & 0 & 0 & 0 \\ 0 & 0 & 0 & 0 & -\mu_v(1-\mathscr{R}_m) & \alpha_v & \alpha_v \\ 0 & 0 & 0 & 0 & 0 & -A_4 & 0 \\ 0 & 0 & 0 & 0 & 0 & \nu_v & -\mu_v \end{pmatrix}$$

The set of eigenvalues for the Jacobian (J_{mf}) is $\{-\mu_h,-A_1,-A_2,-A_3,-\mu_v(1-\mathscr{R}_m),-A_4,-\mu_v\}$. All eigenvalues are real and negative if $\mathscr{R}_m<1$. Hence, the mosquito-free equilibrium (E_{mf}) is locally asymptotically stable if the vectorial reproduction number is smaller than one and unstable if it is bigger than one. Furthermore, it can be shown that E_{mf} is globally asymptotically stable if $\mathscr{R}_m\le 1$. Specifically, consider the linear Lyapunov function $\mathscr{L}=\frac{1}{\mu_v}N_v$. Clearly, $\mathscr{L}>0, \forall N_v\neq 0$ and $\mathscr{L}=0$ only when $N_v=0$. On the other hand, $\dot{\mathscr{L}}=\frac{1}{\mu_v}\dot{N}_v=\frac{1}{\mu_v}\left[\alpha_v\left(1-\frac{N_v}{\kappa_v}\right)-\mu_v\right]N_v=-\left[(1-\mathscr{R}_m)+\frac{N_v}{\kappa_v}\mathscr{R}_m\right]N_v<0$ if $\mathscr{R}_m\le 1$. By LaSalles invariance principle the mosquito-free equilibrium solution (E_{mf}) is globally asymptotically stable whenever $\mathscr{R}_m\le 1$.

3.1.3. Stability of the disease-free equilibrium

The Jacobian of the model (2.1) at the disease-free equilibrium is

$$J_{df}(E_{df})=\begin{pmatrix} -\mu_h & 0 & \gamma_h & \rho_h & 0 & 0 & -\beta_v p_{vh} \\ 0 & -A_1 & 0 & 0 & 0 & 0 & \beta_v p_{vh} \\ 0 & \nu_h & -A_2 & 0 & 0 & 0 & 0 \\ 0 & 0 & \sigma_h & -A_3 & 0 & 0 & 0 \\ 0 & 0 & \frac{G_1G_2}{\Lambda_h\alpha_v} & \frac{\epsilon_r G_1G_2}{\Lambda_h\alpha_v} & G_2 & G_3 & G_3 \\ 0 & 0 & -\frac{G_1g_2}{\Lambda_h\alpha_v} & -\frac{\epsilon_r G_1G_2}{\Lambda_h\alpha_v} & 0 & -A_4 & 0 \\ 0 & 0 & 0 & 0 & 0 & \nu_v & -\mu_v \end{pmatrix},$$

where $G_1=\beta_v p_{hv}\mu_h\kappa_v, G_2=\mu_v\left(1-\mathscr{R}_m\right), G_3=\mu_v\left(2-\mathscr{R}_m\right)$. Eigenvalues ($\zeta$) of the Jacobian ($J_{df}$) can be determined from the matrix equation $|J_{df}-\zeta I_7|=0$, where I_7 is the 7 by 7 identity matrix and $\mathscr{R}_m>1$. This leads to the polynomial characteristic equation:

$$(\zeta+\mu_h)[\zeta+\mu_v\left(\mathscr{R}_m-1\right)](\zeta^5+B_4\zeta^4+B_3\zeta^3+B_2\zeta^2+B_1\zeta+B_0)=0, \tag{3.2}$$

where

$$\begin{aligned} B_4 &= \mu_v+A_1+A_2+A_3+A_4, \\ B_3 &= \mu_v(A_1+A_2+A_3+A_4)+A_1(A_2+A_3+A_4)+A_2(A_3+A_4)+A_3A_4, \\ B_2 &= \mu_v\left[A_1\left(A_2+A_3+A_4\right)+A_2\left(A_3+A_4\right)+A_3A_4\right] \\ &\quad +A_1\left[A_2\left(A_3+A_4\right)+A_3A_4\right]+A_2A_3A_4, \\ B_1 &= \mu_v\left\{A_1\left[A_2\left(A_3+A_4\right)+A_3A_4\right]+A_2A_3A_4\right\} \\ &\quad +A_1A_2A_3A_4\left(1-\mu_vR_c^2\right)>0 \text{ if } R_c<1, \\ B_0 &= \mu_vA_1A_2A_3A_4\left(1-R_c^2\right)>0, \text{ if } R_c<1. \end{aligned}$$

From Eq. (3.2), the first two eigenvalues, $-\mu_h$ and $-\mu_v(\mathscr{R}_m-1)$, are both negative since $\mathscr{R}_m>1$, otherwise the vector population will become extinct. Hence, the local stability of the disease-free equilibrium can be determined from the fifth-degree polynomial component of Eq. (3.2). To this effect, all the coefficients ($B_i, i=1,2,3,4$) of the fifth-degree polynomial component of Eq. (3.2) are greater than zero when $R_c<1$. Therefore, from Descartes Rule of signs, there is no sign change in the sequence of coefficients and so the polynomial cannot have a positive root. That is, when $R_c<1$, all eigenvalues of the Jacobian (J_{df}) are negative (if they are real) or have negative real parts (if they are complex). This implies that the disease-free equilibrium is locally asymptotically stable when $R_c<1$ and unstable when $R_c>1$.

Table 3
A summary of conditions for the existence of endemic equilibria and the possible number of equilibria to System (2.1). The system can possess zero or two endemic equilibrium point(s) when $R_1 \leq 1$ and one endemic equilibrium point when $R_c > 1$.

Case	R_c	R_1	Possible number of equilibria
1	$R_c \leq 1$	$R_1 \leq 1$	0
2	$R_c > 1$	$R_1 \leq 1$	1
3	$R_c \geq 1$	$R_1 > 1$	1
4	$R_c < 1$	$R_1 > 1$	0 or 2

3.1.4. Endemic equilibria and backward bifurcation

The dynamics of the model (2.1) with constant ITN efficacy and no temperature effects is studied in the presence of malaria. Endemic equilibria $E_e^* = (S_h^*, E_h^*, I_h^*, R_h^*, S_v^*, E_v^*, I_v^*)$, of the model are given by

$$S_h^* = \frac{\Lambda_h A_1 A_2 A_3}{\mu_h A_1 A_2 A_3 + A_5 \lambda_{vh}^*}, E_h^* = \frac{\Lambda_h A_2 A_3 \lambda_{vh}^*}{\mu_h A_1 A_2 A_3 + A_5 \lambda_{vh}^*}, I_h^* = \frac{\Lambda_h \nu_h A_3 \lambda_{vh}^*}{\mu_h A_1 A_2 A_3 + A_5 \lambda_{vh}^*},$$
$$R_h^* = \frac{\Lambda_h \nu_h \sigma_h \lambda_{vh}^*}{\mu_h A_1 A_2 A_3 + A_5 \lambda_{vh}^*}, N_h^* = S_h^* + E_h^* + I_h^* + R_h^* = \frac{\Lambda_h (A_1 A_2 A_3 + A_6 \lambda_{vh}^*)}{\mu_h A_1 A_2 A_3 + A_5 \lambda_{vh}^*},$$
$$S_v^* = \frac{\kappa_v \mu_v^2 (\mathscr{R}_m - 1)}{\alpha_v (\lambda_{hv}^* + \mu_v)}, E_v^* = \frac{\kappa_v \mu_v^2 (\mathscr{R}_m - 1) \lambda_{hv}^*}{\alpha_v A_4 (\lambda_{hv}^* + \mu_v)}, I_v^* = \frac{\kappa_v \mu_v \nu_v (\mathscr{R}_m - 1) \lambda_{hv}^*}{\alpha_v A_4 (\lambda_{hv}^* + \mu_v)},$$

where $A_5 = \mu_h \left(A_2 A_3 + \nu_h \sigma_h\right) + \nu_h \left(\delta_h + \mu_h\right) A_3$, $A_6 = (A_2 A_3 + \nu_h (A_3 + \sigma_h))$, and λ_{vh}^* and λ_{hv}^* are the equilibrium values of λ_{vh} and λ_{hv}, respectively.

$$\lambda_{vh}^* = \frac{\beta p_{vh} \kappa_v \nu_v [A_1 A_2 A_3 (\lambda_{vh}^* + \mu_h) - \nu_h (\gamma_h A_3 + \rho_h \sigma_h) \lambda_{vh}^*]}{\alpha_v A_4 A_h \{A_1 A_2 A_3 + [A_2 A_3 + \nu_h (A_3 + \sigma_h)] \lambda_{vh}^*\}} \frac{\lambda_{hv}^*}{\lambda_{hv}^* + \mu_v}, \quad (3.3)$$

$$\lambda_{hv}^* = \frac{\beta p_{hv} (I_h^* + \epsilon_r R_h^*)}{N_h^*} = \frac{\beta p_{hv} \nu_h (A_3 + \epsilon_r \sigma) \lambda_{vh}^*}{A_1 A_2 A_3 + [A_2 A_3 + \nu_h (A_3 + \sigma_h)] \lambda_{vh}^*}. \quad (3.4)$$

Substituting Eq. (3.4) in Eq. (3.3) and simplifying leads to the equation:

$$(\lambda_{vh}^{*2} + C_1 \lambda_{vh}^* + C_0) \lambda_{vh}^* = 0, \quad (3.5)$$

where

$$C_1 = \frac{A_1 A_2 A_3 [\beta p_{hv} \nu_h (A_3 + \epsilon_r \sigma_h)] + 2 \mu_v A_6}{A_6 [\beta p_{hv} \nu_h (A_3 + \epsilon_r \sigma_h) + \mu_v A_6]} (1 - R_1),$$
$$C_0 = \frac{\mu_v (A_1 A_2 A_3)^2}{A_6 [\beta p_{hv} \nu_h (A_3 + \epsilon_r \sigma_h) + \mu_v A_6]} (1 - R_c^2),$$
$$R_1 = \frac{\beta^2 p_{hv} p_{vh} \nu_h \nu_v A_0 A_5}{\mu_h \{\alpha_v A_h A_1 A_2 A_3 A_4 [\beta p_{hv} \nu_h (A_3 + \epsilon_r \sigma_h)] + 2 \mu_v A_6\}}.$$

Conditions for the existence of endemic equilibria and the possible number of endemic equilibria to the model (2.1) with constant ITN efficacy and no temperature effects are given in Table 3 and Theorem 3.1.

The model (2.1) when $\varepsilon_\beta = \varepsilon_{\mu_v} = \varepsilon_0$ is constant can have zero or two endemic equilibrium point(s) when $R_0 \leq 1$, and one endemic equilibrium when $R_0 > 1$. This is summarized in the following result:

Theorem 3.1. *When $\varepsilon_\beta = \varepsilon_{\mu_v} = \varepsilon_0$ is constant, the model (2.1) can have*

(a) *no endemic equilibrium when $R_c \leq 1$ and $R_1 \leq 1$;*
(b) *one endemic equilibrium if $R_c > 1$ and $R_1 \leq 1$ or $R_c \geq 1$ and $R_1 > 1$.*
(c) *zero or two possible endemic equilibrium points if $R_c < 1$ and $R_1 > 1$.*

The case in which the model has no endemic equilibrium point is illustrated in Fig. S1 (a) and (d) of the SI, while the case in which the model has a single endemic equilibrium point is illustrated in Fig. S1 (b)–(c) and (e)–(f) of the SI. Part (c) of Theorem 3.1 indicates that the model might have two endemic equilibria when the reproduction number (R_c) is below one. Thus, there is a parameter regime under which the model might exhibit a sub-critical (backward) bifurcation (Fig. 2). This is a dynamic process that is characterized by the coexistence of a stable disease-free and a stable endemic equilibrium when the associated reproduction number of the model is less than one [79–81]. In this case, the critical value of the reproduction number that is necessary for disease elimination (i.e., below which the reproduction number must be reduced further to achieve elimination) is given by

$$R_c^{bb} = \sqrt{1 - \frac{A_6 (\beta p_{hv} \nu_h (\epsilon_r \sigma_h + A_3) + \mu_v A_6) C_1^2}{4 \mu_v (A_1 A_2 A_3)^2}}. \quad (3.6)$$

3.2. Simulation results for the cases with constant and waning ITN-efficacy and constant or no temperature effects

In this section, the model (2.1) will be simulated to assess the impact of decay in ITN-efficacy and temperature on the dynamics of malaria. In all cases, unless otherwise specified, the simulations are performed using the baseline parameter values presented in Tables 1–2.

3.2.1. Forward versus backward bifurcation

Theorem 3.1 indicates that when the efficacy of ITNs is constant over time (i.e., when $\varepsilon_\beta = \varepsilon_{\mu_v} = \varepsilon_0$), and each of the temperature-dependent parameters (i.e., $\phi_e, \xi_e, p_e, \beta, \nu_v$, and μ_{v0}) is constant, the model (2.1) can have a unique endemic equilibrium when $R_c > 1$ or two possible endemic equilibria when $R_c < 1$. Thus, when $R_c < 1$, the model (2.1) can exhibit a subcritical (backward) bifurcation under certain parameter conditions [79–81]. It was established in [39] that this phenomenon occurs in this class of models with ITN-use when the human malaria-related mortality rate (δ_h) exceeds the human natural mortality rate (μ_h). The model (2.1) is simulated to illustrate the possibility of a forward bifurcation when $\delta_h = 32.9/(365 \times 10^3) < \mu_h$ (Fig. 2(a)–(c)) and a backward bifurcation when $\delta_h = 32.9/(365 \times (10^2)/2) > \mu_h$ (Fig. 2(a)–(c)). Under the parameter regime for which the model (2.1) exhibits a backward bifurcation, the new threshold value of the reproduction number required for disease elimination is $R_c^{bb} = 0.74$. Thus, a backward bifurcation occurs for $0.74 = R_c^{bb} < R_c < 1$, while the disease-free equilibrium is globally asymptotically stable when $R_c < R_c^{bb} = 0.74$.

More results for the case with constant ITN-efficacy and no temperature consideration depicting the impact on the control reproduction number (R_c) as a function of the ITN coverage (b_0) of different parameters through which control measures can be assessed (e.g., $\epsilon_0, \beta_u, \gamma_h, \kappa_v, \mu_{v0}, \mu_{v1}, \beta_l, p_{hv}, p_{vh}$, and ν_v) are given in Figs. S2–S3. Also, heat maps of R_c, the equilibrium value of the infectious human population and the total infectious human population as functions of ITN coverage and β_u, κ_v, and μ_{v1} are presented in Fig. S4.

3.2.2. The impact of ITN coverage, ITN efficacy, and ITN-induced mortality

In this Section, the assumption that the efficacy of ITNs is constant is relaxed and the algorithm in [39,82] is used to compute the reproduction number of the continuous periodic disease model system with decaying ITN efficacy and periodic replacement time (i.e., the model described by Eqs. (2.1), (2.4), (2.5), and (2.6)). Following Theorem 2.1 and Lemma 2.2 in [82], computing the reproduction number of this full periodic non-autonomous system entails rewriting the corresponding infection sub-system in the form $\frac{dw}{dt} = \left(-\mathscr{V}(t) + \frac{1}{\zeta}\mathscr{F}(t)\right) w, w \in \mathbb{R}^5$, where $\mathscr{F}$ is the matrix of newly generated infections, $\mathscr{V}$ is the matrix of transitions, $\zeta \in (0, \infty)$ is a parameter, and $W(t, \zeta), t \geq 0$ is the evolution operator of the system. The reproduction number is the spectral radius of $W(T, \zeta)$. See [82] for the full algorithm and [39] for a summary of the algorithm and an application of the algorithm to a malaria model system with decaying ITN efficacy but no temperature consideration. It should be noted that $\mathscr{F}$ and $\mathscr{V}$ are of the same form as in Section 3.1.1 and that due to the complexity of the model, a closed form expression for the reproduction number cannot be obtained. Hence, a numerical profile of the reproduction number as a function of important model parameters is determined and threshold values of these parameters for which the reproduction number is unity are identified. Fig. 3 shows contour plots of the control reproduction number (R_c) of the model (2.1) for the case in which ITN efficacy is constant (Fig. 3(a) and (d)), averaged (Fig. 3(b) and (e)), and declining over time (Fig. 3(c) and (f)) as functions of ITN coverage, b_0, and initial ITN efficacy, ε_0 (Fig. 3(a–c)), as well as ITN coverage and the ITN-induced mortality rate, μ_{v1}

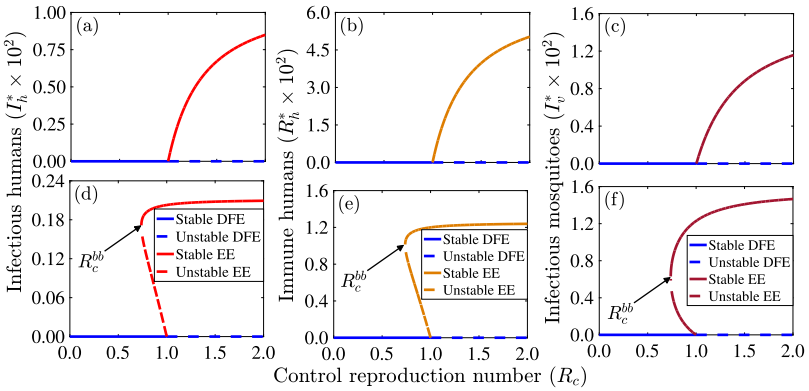

Fig. 2. Numerical simulations of the model (2.1) when ITN efficacy is constant and each of the temperature-dependent parameters is constant showing (a)–(c) a forward bifurcation when the disease-induced death rate is less than the natural death rate (i.e., $\delta_h = 32.9/(365\times10^3) < \mu_h$) and (d)–(f) a backward bifurcation when $\delta_h = 32.9/(365\times(10^2)/2) > \mu_h$. The value of the threshold (R_c^{bb}) is 0.74, and the other parameter values used for the simulations are given in Table 1.

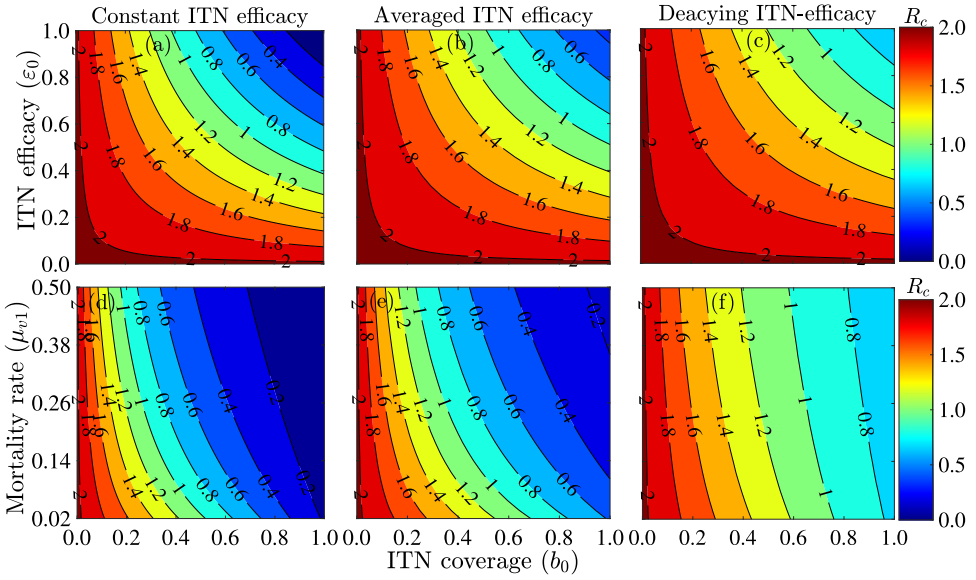

Fig. 3. Contour plots of the control reproduction number (R_c) of the model (2.1) for the case in which ITN efficacy is constant over time ((a) and (d)), time-averaged ((c) and (e)), and decays over time ((c) and (f)). Each reproduction number is plotted as a function of ITN coverage and the initial efficacy of ITNs ((a)–(c)), and as a function of ITN coverage and ITN-related killing rate of mosquitoes ((d)–(f)). The other parameters used for producing the plots are given in Tables 1–2.

(Fig. 3(d–f)). The figure shows that if ITN coverage is maintained at the baseline value of 43% reported by the World Health Organization [5], then malaria elimination is impossible if ITN efficacy is averaged or decays over time. However, if the initial ITN efficacy and the ITN-related killing rate of mosquitoes are held at their baseline levels (given in Table 1), then Fig. 3 indicates that ≈ 43% ITN coverage is required to reduce R_c below one if ITN efficacy is constant over time (Fig. 3(a) and (d)), ≈ 55% ITN coverage is required if ITN efficacy is averaged (Fig. 3(b) and (e)), while ≈ 72% ITN coverage is required if ITN efficacy declines over time (Fig. 3(c) and (f)). These coverage percentages increase with reductions in the initial ITN efficacy or ITN-induced mortality rate of mosquitoes. In particular, if the efficacy of ITNs drops below 50%, then containing malaria using only ITNs when ITN efficacy is averaged or decaying over time is impossible.

3.2.3. *Assessing the impact of ITN coverage, lifespan, and replacement time*

The World Health Organization recommended a transition from regular insecticide-impregnated nets to long-lasting insecticidal nets (that can retain their effectiveness and durability for up to 3 years) in order to minimize issues associated with re-impregnating nets with insecticides or replacing nets frequently [83,84]. Fig. 4 depicts a contour plot of the control reproduction number of the model (2.1) with decaying ITN efficacy and periodic ITN replacement time as a function of ITN coverage and the lifespan of ITNs (Fig. 4(a)), as well as a contour plot of the control reproduction number of the model (2.1) as a function of ITN coverage and the effective replacement time of ITNs (Fig. 4(b)). As in [39,40], the results indicate that ITNs with longer lifespans outperform those with shorter lifespans in malaria control. In particular, if the lifespan of ITNs is as short as one year, then containing malaria only through ITN-use is impossible even if everybody in the community sleeps under ITNs. For ITNs with a lifespan of 3 years, ≈ 74% ITN coverage is required to contain malaria, while for ITNs with a lifespan of 5 years, only ≈ 54% ITN coverage is required to contain malaria (Fig. 4(a)). On the other hand, replacing ITNs before the end of their useful lifespan performs better in malaria control than after their lifespans. For example, if ITNs with a useful life of 3 years are replaced after 2 years, ≈ 58% ITN coverage is required for containing malaria, while if the ITNs are replaced after 4 years, ≈ 88% (i.e., an additional 30%) ITN coverage is required to contain the disease (Fig. 4(b)). To

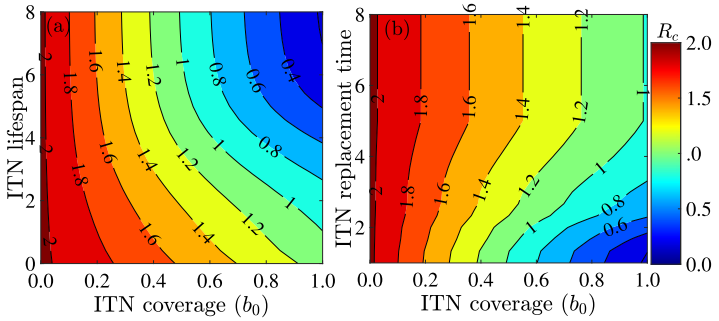

Fig. 4. Contour plots of the control reproduction number of the model (2.1) with decaying ITN efficacy and periodic ITN replacement time as a function of ITN coverage and (a) the lifespan of ITNs, and (b) the effective replacement time of ITNs. The other parameters used for producing the plots are given in Tables 1–2.

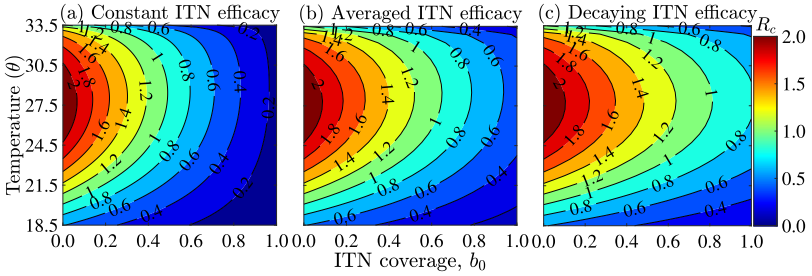

Fig. 5. Contour plot of the control reproduction number of the model (2.1) as a function of ITN coverage and temperature for the case with (a) constant ITN efficacy, (b) averaged ITN efficacy, and (c) decaying ITN efficacy with periodic replacement time. The other parameters used for producing the plots are given in Tables 1–2.

summarize, ITNs with longer usable durations that are replaced before the useful lifetime expires are recommended for malaria control.

3.2.4. Assessing the impact of ITN coverage and temperature

To assess the impact of ITN coverage and temperature on the dynamics of malaria, a contour plot of the control reproduction number of the model (2.1) as a function of ITN coverage and temperature for the scenario with constant, averaged, and decaying ITN efficacy is produced (Fig. 5). The results obtained show that malaria transmission is optimized at temperatures of ≈28°C if there is no ITN coverage (i.e., $b_0 = 0$). The value of the control reproduction number in this case is $R_c \approx 2.2$. For this scenario in which $\theta \approx 28$°C, at least a 49% ITN coverage is required to reduce the control reproduction number below one when the efficacy of ITNs is constant (Fig. 5(a)). For temperatures that are lower or greater than this optimum, lower ITN coverage levels are required. For example, a 42% ITN coverage is required to reduce the control reproduction number below one when the temperature is 25°C or ≈32°C (Fig. 5(a)). Higher ITN coverage levels are required for the case with time-averaged ITN efficacy to reduce R_c below one. For example, when $\theta \approx 28$°C, at least a 69% ITN coverage is required (Fig. 5(b)). Even higher ITN coverage levels are required for the case with decaying ITN efficacy. In particular, at least 81% ITN coverage is required to reduce R_c below one if $\theta \approx 28$°C, while 71% ITN coverage is required if $\theta \approx 25$°C or $\theta \approx 31$°C (Fig. 5(c)). Hence, the ITN coverage required to contain the malaria disease is underestimated by ≈ 32% for the temperature at which transmission is maximized (comparing the cases for constant ITN efficacy in Fig. 5(a) and decaying ITN efficacy in Fig. 5(c)). In summary, this result shows that at temperatures in which malaria transmission is maximized, more ITN coverage is required to contain the disease and that not taking into account waning of ITN efficacy underestimates the control effort required to contain malaria.

3.2.5. The impact of temperature and some control-related parameters

As shown in [34,47] and Figs. S5–S6 of the SI, temperature-dependent parameters of the model (2.1) and some model outcomes (e.g., the reproduction number) as functions of temperature (θ) are unimodal. Consequently, there are ideal temperatures at which these parameters are maximized or minimized. Fig. 6 depicts this unimodal relationship, as well as the impact of temperature, the scaling factor (c_{β_u}) of the temperature response biting rate function, the human recovery rate (γ_h), and the ITN-induced mortality rate of mosquitoes (μ_{v1}) on the control reproduction number of the model (2.1) with decaying ITN efficacy and periodic ITN replacement time. As in Section 3.2.4, the results show that the temperature response of the control reproduction number attains a peak around ≈ 28°C. For this peak temperature, reducing the reproduction number below unity requires the mosquito biting rate scaling factor to be at most $c_{\beta_u} = 1.8 \times 10^{-4}$ (Fig. 6(a)) or $c_{\beta_u} = 1.4 \times 10^{-4}$ (Fig. 6(d)), the human recovery rate to be $\gamma_h = 2.2 \times 10^{-2}$ (Fig. 6(b)) or $\gamma_h = 4.4 \times 10^{-2}$ (Fig. 6(e)), and the ITN-induced mortality rate of mosquitoes to be $\mu_{v1} = 1.2 \times 10^{-1}$ (Fig. 6(c)) or $\mu_{v1} = 3.04$ (Fig. 6(f)), which might not be feasible. However, for a temperature of 24°C or 32°C, for example, reducing the reproduction number below unity requires the mosquito biting rate scaling factor to be at most $c_{\beta_u} = 2.3 \times 10^{-4}$ (Fig. 6(a)) or $c_{\beta_u} = 1.7 \times 10^{-4}$ (Fig. 6(d)), the human recovery rate from infection to be $\gamma_h = 1.3 \times 10^{-2}$ (Fig. 6(b)) or $\gamma_h = 2.8 \times 10^{-2}$ (Fig. 6(e)), and the ITN-induced mortality rate of mosquitoes to be $\mu_{v1} = 0.4 \times 10^{-1}$ (Fig. 6(c)) or $\mu_{v1} = 8.5 \times 10^{-1}$ (Fig. 6(f)).

3.3. Simulations for the case with waning ITN-efficacy and seasonality

In this Section, we assess the impact of waning ITN efficacy and seasonality on the dynamics of malaria transmission. The scenarios considered include a control case of the model (2.1) in which ITN efficacy is constant with no temperature effects, and cases of the model (2.1) in which ITN efficacy wanes with no temperature effects, with temperature effects, and with both temperature effects and seasonality.

3.3.1. Interaction between periodic ITN replacement and seasonality

The model (2.1) with Eqs. (2.4), (2.5) and (2.6) is simulated to assess the impact of temperature on the long-term dynamics of the infectious human and mosquito populations for the cases in which ITN efficacy decays over time with temperature effects and seasonality. In each scenario, ITNs are replaced periodically. The results of the simulations (Fig. 7) show bounded periodic oscillations due to periodic

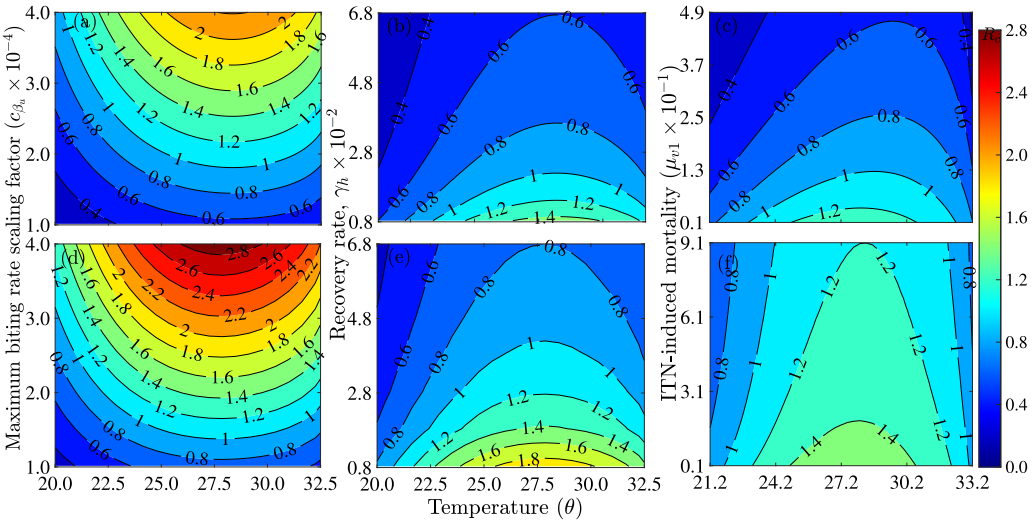

Fig. 6. Contour plots of the control reproduction number of the model (2.1) as functions of temperature and the scaling factor (c_{β_u}) of the temperature response biting rate ((a) and (d)), the human recovery rate from infection, γ_h ((b) and (e)), and the ITN-induced mortality rate of mosquitoes, μ_{v1} ((c) and (f)). (a)–(c): Results for the case with constant ITN efficacy. (d)–(f): Results for the model with decaying ITN efficacy and periodic replacement time. The other parameters used for producing the plots are given in Tables 1–2.

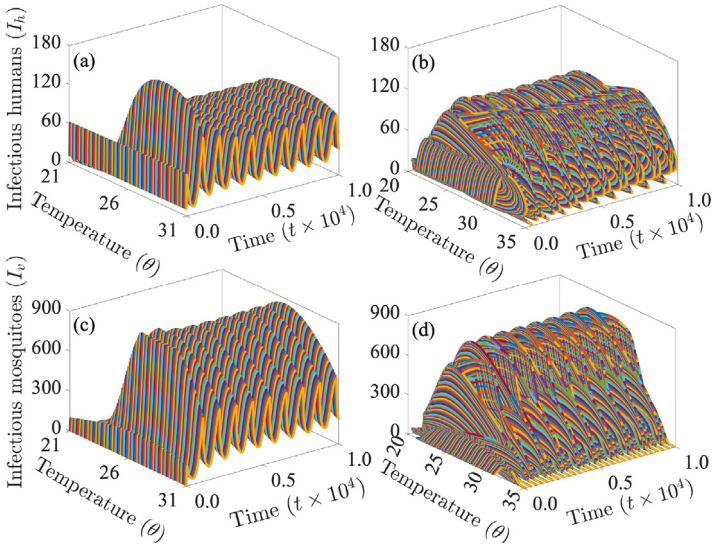

Fig. 7. Long-term dynamics of the model (2.1) showing the effects of temperature on the (a)–(b) infectious human population and (c)–(d) infectious mosquito population for the case with constant temperature ((a) and (c)) and seasonality ((b) and (d)). The values of the other parameters used for the simulations are given in Tables 1–2.

replacement of ITNs for the case with no seasonality (Fig. 7(a) and (c)). Due to interactions between the periodic ITN replacement cycles and seasonality, a major regular oscillation pattern with multiple slightly smaller regular oscillations is observed (Fig. 7(b) and (d)). This highlights the possibility of multiple malaria waves (with slightly smaller waves between major waves). Two-dimensional plots that also include the case with constant ITN efficacy (a stable non-oscillatory endemic equilibrium), and the long-term dynamics of the other model variables are presented in Fig. S7 of the SI.

3.3.2. Global sensitivity analysis

In this Section, a global sensitivity analysis of the model (2.1) is performed following the Latin Hypercube Sampling (LHS) and Partial Rank Correlation Coefficients (PRCCs) procedures outlined in [85] and applied to malaria models with waning ITN-efficacy in [39,40]. A single response function — the total infectious human population (i.e., the human disease burden) is considered for four different scenarios of the model system described by Eqs. (2.1): the case with (a) constant ITN efficacy but no temperature effects, (b) declining ITN efficacy but no temperature effects, (c) declining ITN efficacy and temperature effects, and (d) declining ITN efficacy with temperature effects and temperature fluctuations. The results illustrated in Fig. 8 show that the human recovery rate from infection (γ_h), the maximum biting rate of mosquitoes (β_u), the scaling factor of temperature-dependent biting rate (c_{β_u}), the ITN coverage (b_0), the initial ITN efficacy (ε_0), the probability of an infectious human (mosquito) infecting a susceptible mosquito (human), p_{hv} (p_{vh}), and the mosquito carrying capacity (κ_v) consistently have the greatest impact on the response function for each of the four scenarios. Each of these consistently significant parameters is associated with a malaria control measure. For example, increases (decreases) in b_0 and γ_h, which translate to increased (reduced) ITN coverage and treatment of infectious individuals, respectively, will lead to significant reductions (increases) in disease burden. This confirms the importance of ITNs and treatment in fighting malaria. Also, increases (decreases) in β_u, p_{hv}, p_{vh}, and κ_v will lead to appreciable increases (reductions) in disease burden. For the scenarios with constant temperature and seasonality, temperature (θ) and the annual mean temperature (θ_m) are the most significant parameters (Fig. 8(c)–(d)). This highlights the

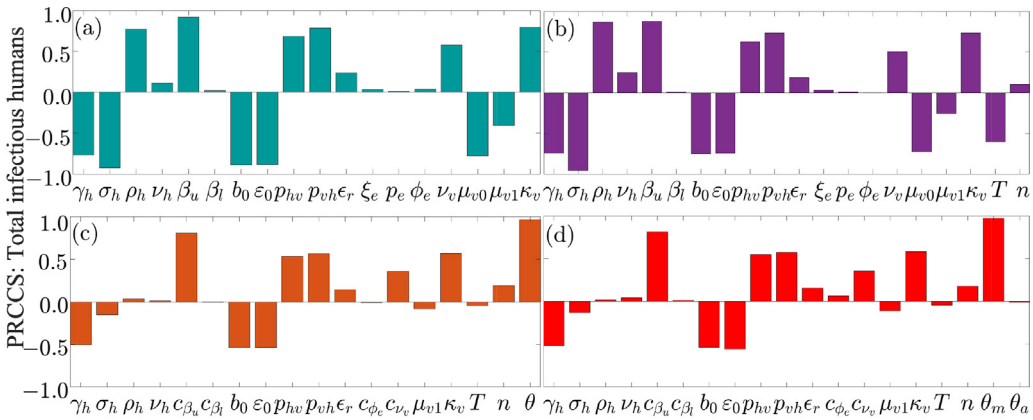

Fig. 8. Global sensitivity analysis results depicting the impact of parameters on the burden of malaria (i.e., the total infectious human population) for the model (2.1) with (a) constant ITN efficacy with no temperature effects, (b) declining ITN efficacy with no temperature effects, (c) declining ITN efficacy with temperature effects, and (d) declining ITN efficacy with temperature effects and temperature fluctuations.

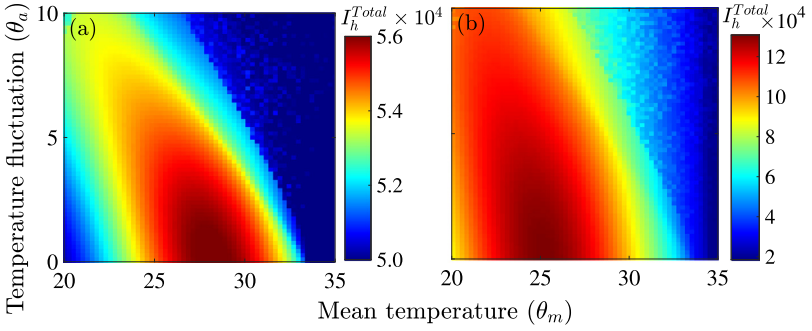

Fig. 9. Simulations of the model (2.1) showing the impact on the total infectious human population (human malaria burden) as a function of the mean annual temperature (θ_m) and the amplitude or seasonal deviation from the mean annual temperature (θ_a) for the scenario with (a) constant ITN efficacy and seasonality and (b) waning ITN efficacy and seasonality. The values of the other parameters used for the simulations are given in Tables 1–2.

significance of temperature as a major driver of malaria transmission. In each of the four scenarios, the minimum biting rate of mosquitoes has the least impact on the total infectious human population. Hence, the risk of contracting malaria is low in regions where the number of mosquitoes is low or where mosquitoes do not bite humans very often.

3.3.3. *Impact of mean annual temperature and temperature fluctuations*

The model (2.1) with Eqs. (2.4)–(2.7) is simulated to assess the impact of mean temperature and temperature fluctuations on peak malaria incidence and the total infectious human population. The simulation is carried out for the scenario with seasonality (i.e., when temperature is defined by Eq. (2.7).) The results of the simulation (presented in Fig. 9) show that the total human malaria burden (i.e., the total infectious human population) is highly sensitive to the annual mean temperature (θ_m) and the seasonal deviation from the mean annual temperature (θ_a). Specifically, with seasonal temperature fluctuations, major malaria outbreaks are possible even at temperatures below and above the annual mean temperature. The range of possible temperatures for which such outbreaks can occur is wider for the model with decaying ITN efficacy and periodic replacement time (Fig. 9(b)) compared to the case with constant ITN efficacy (Fig. 9(a)). In particular with a seasonal temperature fluctuation of 10°C, severe malaria outbreaks can occur in regions with mean temperatures as low as 18°C and as high as 38°C. Accordingly, temperate climates with significant seasonal variation might be able to sustain outbreaks similar to those in tropical climates with less fluctuations in seasonal temperatures. Similar results are obtained if the malaria burden is quantified in terms of the peak incidence (Fig. S8 in the SI). For the case in which ITN efficacy is constant, if the mean annual temperature is held at its baseline value while the temperature fluctuation is 10°C, a 5% reduction in the baseline burden of malaria will be recorded (Fig. 9(a)). However, if the mean temperature is held at the optimal transmission value of 28°C, a temperature fluctuation of ±10°C will lead to an ≈ 8% reduction in the baseline burden of malaria, while no temperature fluctuation will lead to a 3% increase in the baseline burden of malaria (Fig. 9(a)). For corresponding scenarios in the case in which ITN efficacy decays over time, significantly higher percentage reductions are recorded (Fig. 9(b)). For example, if the mean temperature is held at 28°C, a temperature fluctuation of 10°C will lead to an ≈ 43% reduction in the baseline burden of malaria, while no temperature fluctuation will lead to a 3% reduction in the baseline burden of malaria (Fig. 9(b)). Additional heat maps assessing the impact of the burden of malaria as functions of the mean annual temperature (θ_m) and the ITN coverage (b_0), the human recovery rate (γ_h), the scaling factor (c_{β_u}) of the temperature-dependent mosquito-biting rate, and the mosquito carrying capacity (κ_v) are given in Fig. S9 of the SI.

3.3.4. *Assessing the impact of control-related parameters on disease burden*

Fig. 10 depicts heat maps of the human malaria burden as functions of the initial ITN coverage (b_0) and other model parameters through which disease control can be assessed with the exception of the seasonal deviation from the mean annual temperature (θ_a). The heat maps show that if the initial ITN coverage b_0 is held at its baseline value of 43%, while the baseline initial efficacy of ITNs (ε_0) drops to 60%, an 87% increase from the baseline disease burden is recorded (Fig. 10(a)). On the other hand, if the initial ITN coverage is raised to 60%, an 83% reduction from the baseline disease burden is recorded if the initial ITN efficacy is held at its baseline value, while a 25% increase from the baseline disease burden is recorded if the initial ITN efficacy drops to 60% (Fig. 10(a)). High ITN coverage combined with more treatment

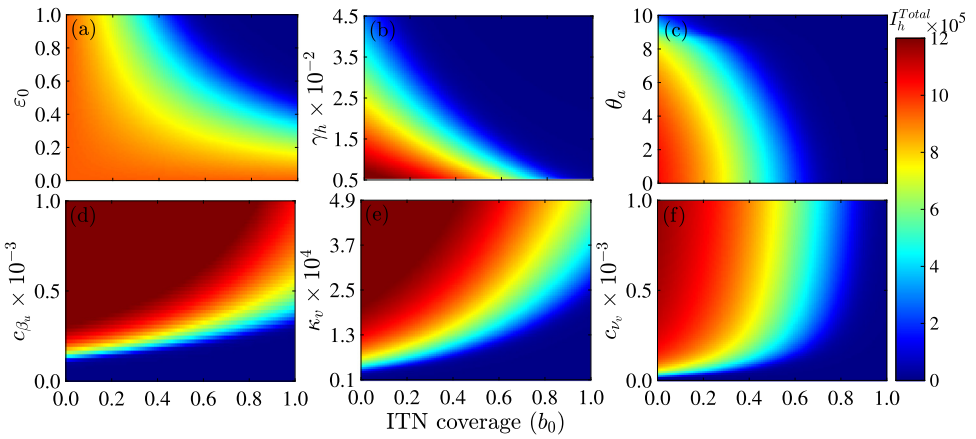

Fig. 10. Heat maps depicting the impact on the human malaria burden (i.e., the total infectious human population) of the ITN coverage (b_0) and the (a) initial ITN efficacy (ε_0), (b) human recovery rate (γ_h), (c) seasonal divergence from the mean annual temperature (θ_a), (d) scaling rate of the temperature-dependent maximum biting rate of mosquitoes (c_{β_u}), (e) carrying capacity of mosquitoes (κ_v), and (f) the scaling rate of the temperature-dependent rate at which exposed humans become infectious (c_{ν_v}). The values of the other parameters are given in Tables 1–2.

of infectious individuals will lead to a significant reduction in malaria burden. In particular, if the initial ITN coverage is held at its baseline value, an 86% increase from the baseline disease burden is recorded if the human recovery rate reduces to 1.2×10^{-2} *per day* from its baseline value in Table 1 (i.e., the average duration of infection increases from 60 to ≈ 86 days), and a 66% reduction in the baseline disease burden is recorded if the baseline human recovery rate is increased by 20%, i.e., to $\gamma_h = 2.2\times10^{-2}$ *per day* or the average duration of infection is 46 days (Fig. 10(b)). But if the baseline initial ITN coverage is increased by 30% (i.e., from 43–56%), an 83% decrease from the baseline disease burden is recorded if the recovery rate is held at its baseline value, while a drastic 93% decrease is recorded if the recovery rate rises by 30% (Fig. 10(b)). More results for other parameters (depicted in Fig. 10(c)–(f)) are illustrated in Table S1 of the SI. Similar results are obtained for the case in which disease burden is quantified in terms of the endemic equilibrium (Fig. S10 of the SI).

4. Discussion and conclusion

Malaria is one of the deadliest and most common diseases of humans that is spread by mosquitoes. It affects humans in many parts of the world, especially humans in tropical and subtropical regions. For example, ≈ 95% of the global malaria cases in 2020 were from Africa, with 55% of these cases from only six countries [5]. Although ITNs have been instrumental in curtailing the transmission of malaria significantly [17], the success of this intervention measure is challenged by many factors including mosquito resistance to insecticides used in ITNs, waning of ITN efficacy, and improper usage. Malaria control is also challenged by environmental factors such as temperature since the malaria vector and parasite are both sensitive to changes in temperature. In particular, temperature is necessary for the growth and survival of the malaria vector and parasite. Hence, acquiring insights into the significance of temperature and the decay in ITN efficacy over time and how these interact with the transmission dynamics of malaria is critical in the design and implementation of more effective control measures. Here, the decay in ITN-efficacy and seasonal changes in temperature are incorporated in a model for malaria and the model is used to assess the role of variation in temperature, decay in ITN efficacy and control-related parameters on malaria prevalence.

The model exhibits a backward bifurcation (i.e., a stable disease-free and a stable endemic state co-exist when the reproduction number of the model is less than one). This phenomenon is associated with important disease control implications. Specifically, the occurrence of a backward bifurcation makes disease control more difficult because the reproduction number must be reduced further even when it is slightly less than one to get the system out of the backward bifurcation regime to a region in which the disease-free equilibrium is globally stable. This implies that control efforts must be stepped up and maintained until the control reproduction number (R_c) falls below the backward bifurcation critical value (R_c^{bb}). That is, containing the disease is feasible when $R_c < R_c^{bb}$. This phenomenon occurs within a parameter regime in which the human disease-induced mortality rate is greater than the human natural mortality rate, which is consistent with findings in [39,40].

Simulations of the model show that when ITN-efficacy is constant, averaged, or waning, containing the disease is impossible if all parameters are held at their baseline values. But, holding the ITN coverage at baseline and modifying the other control-related parameters appropriately can lead to elimination. Also, the simulations show that there is a significant correlation between the longevity of an ITN and its effectiveness in controlling malaria, i.e., long-lived ITNs are more effective in controlling malaria than short-lived ones. Furthermore, the analysis shows that malaria control is improved by replacing ITNs before their intended lifespan. The model with constant or averaged ITN-efficacy underestimates disease burden and the required control effort. These results are consistent with those in [39,40].

The effects on epidemiological metrics such as the control reproduction number (R_c) and the human disease burden of the interaction between temperature and certain parameters of the model system that are affected by disease control measures are examined. These include the human biting rate of mosquitoes (β), the adult mosquito mortality rate (μ_v), the probability of an egg surviving to become an adult mosquito (ν_v), the carrying capacity of mosquitoes (κ_v), the probability of infectious mosquitoes spreading malaria to susceptible humans (p_{vh}), the probability of infectious humans spreading malaria to susceptible mosquitoes (p_{hv}), and the rate at which humans recover from malaria (γ_h). In regions where mosquitoes live longer and bite humans more frequently as is the case in sub-Saharan Africa, malaria transmission is high. This is one of the reasons for which most malaria cases (e.g., 95% of the cases in 2020 [5]) are concentrated in Africa. Personal protection (e.g., through the use of ITNs) can lead to a reduction in the human biting rate of mosquitoes by sheltering humans from mosquitoes and killing mosquitoes that land on ITNs. Spraying the interior of homes with insecticides and using ITNs and adulticides can increase the mortality rate of mosquitoes. Furthermore, larvicides can reduce the probability of an egg surviving to become an adult mosquito, while getting rid of mosquito breeding sites close to human dwellings can lead to a decrease in the carrying capacity of mosquitoes. The rate at which humans recover from the malaria disease (γ_h) can be used to assess the impact of treatment with anti-malaria drugs on malaria prevalence. For example, more treatment will result in an increased recovery rate,

while less treatment will result in a lower recovery rate. Additionally, proper handling and care for ITNs can result in longer useful lifespans of ITNs, which our simulations have shown to have a significant impact in reducing the burden of malaria. Furthermore, transmission-blocking Wolbachia bacteria can be used in bio-control strategies to limit the risk of malaria transmission from infectious mosquitoes to susceptible humans (p_{vh}) [86–88]. Results of the global sensitivity analysis in Section 3.3.2 show that some of these parameters (through which control measures can be assessed, e.g., γ_h, κ_v, p_{vh}, and b_0, ε_0, and β_u in β) consistently have the most significant impact on disease burden across each of the four scenarios under consideration (constant ITN efficacy with no temperature effects, declining ITN efficacy with no temperature effects, declining ITN efficacy with temperature effects, and declining ITN efficacy with temperature effects and temperature fluctuations). That is, changes in these parameters will generate more significant changes in malaria burden.

Local and global sensitivity analyses of the model (2.1) show that the total infectious human population and the control reproduction number are highly sensitive to temperature-related parameters. This highlights the significance of temperature in malaria transmission dynamics and hence the importance of accounting for temperature in malaria models and in the design of malaria control measures. Furthermore, this study shows that accounting for both seasonality and decay in ITN efficacy leads to complex patterns. Specifically, interactions between the periodic ITN replacement cycles and seasonal cycles lead to some sort of a period-2 pattern signaling the possibility of a slightly minor malaria wave following a major wave in certain areas. Also, simulations of the model show that malaria transmission is optimized at temperatures of $\approx 28°$C. The ITN coverage level required to contain the disease is lower at temperatures that are lower or higher than this optimum temperature. However, transient temperature changes (i.e., shifts from the annual mean temperature) associated with the seasonal cycle contribute to malaria burden by facilitating or preventing transmission. Specifically, if there is sufficient seasonal variation in temperatures, serious malaria outbreaks are possible in regions with low annual mean temperatures or temperatures below the optimal temperature for malaria transmission. This would be the case in temperate and subtropical climatic zones. For example, in regions with annual mean temperatures of $\approx 18°$C, seasonal temperature variations of $+10°$C can lead to conducive conditions for optimal transmission of malaria.

This study is based on a model that relies on some assumptions. One of the key assumptions is that all ITNs are replaced simultaneously. Furthermore, the study does not take into consideration the role of human decision-making related to the use of ITNs, which can provide valuable information for public health. Although only the effect of temperature is accounted for in this study, other environmental factors such as humidity and precipitation can also impact the dynamics of malaria. Accounting for these factors might alter the results reported here. Despite these limitations, this study identifies important parameters that can be targeted for control purposes and shows that accounting for waning in ITN-efficacy is important in understanding malaria transmission risk and in estimating the effort required to contain malaria. Hence, malaria control strategies must include education on proper handling and use of ITNs. The study shows that malaria is extremely sensitive to seasonal changes in temperature. Specifically, disease burden and the control reproduction number are highly sensitive to temperature-related parameters highlighting the significance of temperature in malaria dynamics. Furthermore, the study shows that malaria transmission risk is optimal at temperatures of 28°C and that major malaria epidemics can emerge even in regions with low temperatures provided seasonal fluctuations in temperature are significantly large. Thus, understanding interactions between malaria dynamics, temperature changes, and waning ITN-efficacy is essential in assessing the impact of temperature variations on malaria risk and in designing improved malaria control and mitigation strategies.

Declaration of competing interest

The authors declare that they have no known competing financial interests or personal relationships that could have appeared to influence the work reported in this paper.

Data availability

No data was used for the research described in the article.

Acknowledgment

CNN acknowledges the support of the Simons Foundation (Award #627346) and the National Science Foundation (Grant Number: DMS #2151870).

Appendix A. Supplementary data

Supplementary material related to this article can be found online at https://doi.org/10.1016/j.mbs.2022.108936.

References

[1] I. Udeinya, J. Schmidt, M. Aikawa, L. Miller, I. Green, Falciparum malaria infected erythrocytes specifically bind to cultured human endothelial cells, Science 80 (213) (1981) 555–557.
[2] J.L. Gallup, J.D. Sachs, The economic burden of malaria, Am. J. Tropical Med. Hygiene 64 (1_suppl) (2001) 85–96.
[3] J. Sachs, P. Malaney, The economic and social burden of malaria, Nature 415 (6872) (2002) 680–685.
[4] World Health Organization, World Malaria Report 2019, World Health Organization, 2020, Assessed on July 10, 2020, URL https://www.who.int/publications/i/item/world-malaria-report-2019.
[5] World Health Organization (WHO), World malaria report 2021, World Health Organization, Geneva, 2021, Assessed on December 16, 2021, URL https://www.who.int/teams/global-malaria-programme/reports/world-malaria-report-2021.
[6] World Health Organization (WHO), World malaria report 2020, World Health Organization, Geneva, 2021, Assessed on December 16, 2021, URL https://www.who.int/publications/i/item/9789240015791.
[7] R.W. Steketee, C.C. Campbell, Impact of national malaria control scale-up programmes in Africa: magnitude and attribution of effects, Malar. J. 9 (1) (2010) 1–15.
[8] K. Karunamoorthi, Vector control: a cornerstone in the malaria elimination campaign, Clin. Microbiol. Infection 17 (11) (2011) 1608–1616.
[9] C. Lengeler, Insecticide-treated bed nets and curtains for preventing malaria, Cochrane Database Syst. Rev. (2) (2004).
[10] F. Nosten, N.J. White, Artemisinin-based combination treatment of *falciparum* malaria, Defining and Defeating the Intolerable Burden of Malaria III: Progress and Perspectives: Supplement To Volume 77 (6) of American Journal of Tropical Medicine and Hygiene (2007).
[11] R.T. Eastman, D.A. Fidock, Artemisinin-based combination therapies: a vital tool in efforts to eliminate malaria, Nat. Rev. Microbiol. 7 (12) (2009) 864–874.
[12] K. Kayentao, M. Kodio, R.D. Newman, H. Maiga, D. Doumtabe, A. Ongoiba, D. Coulibaly, A.S. Keita, B. Maiga, M. Mungai, et al., Comparison of intermittent preventive treatment with chemoprophylaxis for the prevention of malaria during pregnancy in Mali, J. Infect. Dis. 191 (1) (2005) 109–116.
[13] G.F. Killeen, T.A. Smith, H.M. Ferguson, H. Mshinda, S. Abdulla, C. Lengeler, S.P. Kachur, Preventing childhood malaria in Africa by protecting adults from mosquitoes with insecticide-treated nets, PLoS Med. 4 (7) (2007).
[14] A. Enayati, J. Lines, R. Maharaj, J. Hemingway, Suppressing the vector, in: Shrinking the Malaria Map: A Prospectus on Malaria Elimination, Chapter 9, The Global Health Group, Global Health Sciences, University of California, San Francisco, San Francisco, 2009.
[15] B. Greenwood, Control to elimination: implications for malaria research, Trends Parasitol. 24 (2008) 449–454.
[16] K. Mendis, A. Rietveld, M. Warsame, A. Bosman, B. Greenwood, W. Wernsdorfer, From malaria control to eradication: The WHO perspective, Trop. Med. Int. Health 4 (2009) 802–809.
[17] S. Bhatt, D. Weiss, E. Cameron, D. Bisanzio, B. Mappin, U. Dalrymple, K. Battle, C. Moyes, A. Henry, P. Eckhoff, et al., The effect of malaria control on plasmodium falciparum in africa between 2000 and 2015, Nature 526 (7572) (2015) 207–211.
[18] L.H.D. Briët, T. Smith, Importance of factors determining the effective lifetime of a mass, long-lasting, insecticidal net distribution: a sensitivity analysis, Malar. J. 11 (2012) 20.

[19] M. Kayedi, J. Lines, A. Haghdoost, M. Vatandoost, Y. Rassi, K. Khamisabady, Evaluation of the effects of repeated hand washing, sunlight, smoke and dirt on the persistence of deltamethrin on insecticide-treated nets, Trans. R. Soc. Trop. Med. Hyg. 102 (8) (2008) 811–816.

[20] R. Short, R. Gurung, M. Rowcliffe, N. Hill, E. Milner-Gulland, The use of mosquito nets in fisheries: a global perspective, PloS One 13 (1) (2018) e0191519.

[21] K. Honjo, L.F. Chaves, A. Satake, A. Kaneko, N. Minakawa, When they don't bite, we smell money: understanding malaria bednet misuse, Parasitology 140 (5) (2013) 580–586.

[22] H.E. Atieli, G. Zhou, Y. Afrane, M.-C. Lee, I. Mwanzo, A.K. Githeko, G. Yan, Insecticide-treated net (itn) ownership, usage, and malaria transmission in the highlands of western kenya, Parasites & vectors 4 (1) (2011) 1–10.

[23] N. Minakawa, G.O. Dida, G.O. Sonye, K. Futami, S. Kaneko, Unforeseen misuses of bed nets in fishing villages along Lake Victoria, Malaria Journal 7 (1) (2008) 1–6.

[24] E. Lyimo, W. Takken, J. Koella, Effect of rearing temperature and larval density on larval survival, age at pupation and adult size of *Anopheles gambiae*, Entomol. Exp. Et Applicata 63 (3) (1992) 265–271.

[25] M.N. Bayoh, S.W. Lindsay, Effect of temperature on the development of the aquatic stages of *Anopheles gambiae sensu stricto* (Diptera: Culicidae), Bull. Entomol. Res. 93 (5) (2003) 375–381.

[26] M.N. Bayoh, S.W. Lindsay, Temperature-related duration of aquatic stages of the Afrotropical malaria vector mosquito *Anopheles gambiae* in the laboratory, Med. Vet. Entomol. 18 (2) (2004) 174–179.

[27] L.M. Beck-Johnson, W.A. Nelson, K.P. Paaijmans, A.F. Read, M.B. Thomas, O.N. Bjørnstad, The effect of temperature on *Anopheles* mosquito population dynamics and the potential for malaria transmission, PLoS One 8 (11) (2013) e79276.

[28] C.L. Lyons, M. Coetzee, S.L. Chown, Stable and fluctuating temperature effects on the development rate and survival of two malaria vectors, *Anopheles arabiensis* and *Anopheles funestus*, Parasites & Vectors 6 (1) (2013) 1–9.

[29] L.L. Shapiro, S.A. Whitehead, M.B. Thomas, Quantifying the effects of temperature on mosquito and parasite traits that determine the transmission potential of human malaria, PLoS Biol. 15 (10) (2017) e2003489.

[30] K.P. Paaijmans, A.F. Read, M.B. Thomas, Understanding the link between malaria risk and climate, Proc. Natl. Acad. Sci. 106 (33) (2009) 13844–13849.

[31] P.E. Parham, J. Waldock, G.K. Christophides, D. Hemming, F. Agusto, K.J. Evans, N. Fefferman, H. Gaff, A. Gumel, S. LaDeau, et al., Climate, environmental and socio-economic change: weighing up the balance in vector-borne disease transmission, Philos. Trans. R. Soc. B 370 (1665) (2015) 20130551.

[32] M. Yasuno, R.J. Tonn, A study of biting habits of *Aedes aegypti* in Bangkok, Thailand, Bull. World Health Organization 43 (2) (1970) 319.

[33] K.P. Paaijmans, L.J. Cator, M.B. Thomas, Temperature-dependent pre-bloodmeal period and temperature-driven asynchrony between parasite development and mosquito biting rate reduce malaria transmission intensity, PLoS One 8 (1) (2013) e55777.

[34] E.A. Mordecai, K.P. Paaijmans, L.R. Johnson, C. Balzer, T. Ben-Horin, E. de Moor, A. McNally, S. Pawar, S.J. Ryan, T.C. Smith, et al., Optimal temperature for malaria transmission is dramatically lower than previously predicted, Ecol. Lett. 16 (1) (2013) 22–30.

[35] N. Chitnis, A. Schapira, T. Smith, R. Steketee, Comparing the effectiveness of malaria vector-control interventions through a mathematical model, Am. J. Trop. Med. Hyg. 83 (2) (2010) 230–240.

[36] L.C. Okell, L.S. Paintain, J. Webster, K. Hanson, J. Lines, From intervention to impact: modelling the potential mortality impact achievable by different long-lasting, insecticide-treated net delivery strategies, Malar. J. 11 (1) (2012) 327.

[37] O.J. Briët, D. Hardy, T.A. Smith, Importance of factors determining the effective lifetime of a mass, long-lasting, insecticidal net distribution: a sensitivity analysis, Malar. J. 11 (1) (2012) 20.

[38] F. Agusto, S. Valle, K. Blayneh, C. Ngonghala, M. Goncalves, N. Li, R. Zhao, H. Gong, The impact of bed-net use on malaria prevalence, J. Theoret. Biol. 320 (2013) 58–65.

[39] C.N. Ngonghala, S.Y. Del Valle, R. Zhao, J. Mohammed-Awel, Quantifying the impact of decay in bed-net efficacy on malaria transmission, J. Theoret. Biol. 363 (2014) 247–261.

[40] C.N. Ngonghala, J. Mohammed-Awel, R. Zhao, O. Prosper, Interplay between insecticide-treated bed-nets and mosquito demography: implications for malaria control, J. Theoret. Biol. 397 (2016) 179–192.

[41] C.N. Ngonghala, J. Wairimu, J. Adamski, H. Desai, Impact of adaptive mosquito behavior and insecticide-treated nets on malaria prevalence, J. Biol. Systems 28 (02) (2020) 515–542.

[42] C.N. Ngonghala, Assessing the impact of insecticide-treated nets in the face of insecticide resistance on malaria control, J. Theoret. Biol. 555 (2022) 111281.

[43] K. Okuneye, A.B. Gumel, Analysis of a temperature-and rainfall-dependent model for malaria transmission dynamics, Math. Biosci. 287 (2017) 72–92.

[44] S.E. Eikenberry, A.B. Gumel, Mathematical modeling of climate change and malaria transmission dynamics: a historical review, J. Math. Biol. 77 (4) (2018) 857–933.

[45] P.E. Parham, E. Michael, Modeling the effects of weather and climate change on malaria transmission, Environ. Health Perspect. 118 (5) (2010) 620–626.

[46] S. Lindsay, M. Birley, Climate change and malaria transmission, Ann. Trop. Med. Parasitol. 90 (5) (1996) 573–588.

[47] C.N. Ngonghala, S.J. Ryan, B. Tesla, L.R. Demakovsky, E.A. Mordecai, C.C. Murdock, M.H. Bonds, Effects of changes in temperature on Zika dynamics and control, J. R. Soc. Interface 18 (178) (2021) 20210165.

[48] S.E. Clarke, C. Bøgh, R.C. Brown, M. Pinder, G.E. Walraven, S.W. Lindsay, Do untreated bednets protect against malaria? Trans. R. Soc. Trop. Med. Hyg. 95 (5) (2001) 457–462.

[49] World Bank Data, Life Expectancy at Birth, Total (Years) - Sub-Saharan Africa, World Bank, 2020, Accessed on January 3, 2020.

[50] L. Molineaux, G. Gramiccia, The Garki Project: Research on the Epidemiology and Control of Malaria in the Sudan Savanna of West Africa, World Health Organization, Geneva, 1980.

[51] H. Mehlhorn, Encyclopedic Reference of Parasitology: Diseases, Treatment, Therapy, Vol. 2, Springer Science & Business Media, 2001.

[52] N. Chitnis, J.M. Hyman, J.M. Cushing, Determining important parameters in the spread of malaria through the sensitivity analysis of a mathematical model, Bull. Math. Biol. 70 (5) (2008) 1272.

[53] J.A. Filipe, E.M. Riley, C.J. Drakeley, C.J. Sutherland, A.C. Ghani, Determination of the processes driving the acquisition of immunity to malaria using a mathematical transmission model, PLoS Comput. Biol. 3 (12) (2007) e255.

[54] G. Davidson, C. Draper, Field studies of some of the basic factors concerned in the transmission of malaria, Trans. R. Soc. Trop. Med. Hyg. 47 (6) (1953) 522–535.

[55] E. Krafsur, J. Armstrong, An integrated view of entomological and parasitological observations on *falciparum* malaria in Gambela, Western Ethiopian Lowlands, Trans. R. Soc. Trop. Med. Hyg. 72 (4) (1978) 348–356.

[56] J. Nedelman, Introductory review some new thoughts about some old malaria models, Math. Biosci. 73 (2) (1985) 159–182.

[57] M.F. Boyd, Epidemiology of malaria: factors related to the intermediate host, in: Malariology, Vol. 1, WB Saunders Philadelphia, 1949, pp. 551–607.

[58] M. Smalley, R. Sinden, *Plasmodium falciparum* gametocytes: their longevity and infectivity, Parasitology 74 (1) (1977) 1–8.

[59] J. Nedelman, Inoculation and recovery rates in the malaria model of Dietz, Molineaux, and Thomas, Math. Biosci. 69 (2) (1984) 209–233.

[60] L. Molineaux, G. Shidrawi, J. Clarke, J. Boulzaguet, T. Ashkar, Assessment of insecticidal impact on the malaria mosquito's vectorial capacity, from data on the man-biting rate and age-composition, Bull. World Health Organization 57 (2) (1979) 265.

[61] S. Gupta, J. Swinton, R.M. Anderson, Theoretical studies of the effects of heterogeneity in the parasite population on the transmission dynamics of malaria, Proc. R. Soc. B 256 (1347) (1994) 231–238.

[62] World Health Organization, Insecticide-treated mosquito nets: A WHO position statement, Glob. Malar. Programme (2007).

[63] World Health Organization, Control of neglected tropical diseases. WHO pesticide evaluation scheme, vector control unit: guidelines for monitoring the durability of long-lasting insecticidal mosquito nets under operational conditions, Glob. Malar. Programme (2011).

[64] A.-M. Pulkki-Brännström, C. Wolff, N. Brännström, J. Skordis-Worrall, Cost and cost effectiveness of long-lasting insecticide-treated bed nets-a model-based analysis, Cost Effectiveness Resour. Allocation 10 (1) (2012) 5.

[65] H. Delatte, G. Gimonneau, A. Triboire, D. Fontenille, Influence of temperature on immature development, survival, longevity, fecundity, and gonotrophic cycles of aedes albopictus, vector of chikungunya and dengue in the Indian ocean, J. Med. Entomol. 46 (1) (2009) 33–41.

[66] J.A. Vaughan, B.H. Noden, J.C. Beier, Population dynamics of *Plasmodium falciparum* sporogony in laboratory-infected *Anopheles gambiae*, J. Parasitol. 78 (4) (1992) 716–724.

[67] H. Giles, D. Warrel, Bruce-Chwatts Essential Malariology, fourth ed., Hodder Arnold, London, 2002.

[68] J. Lines, J. Myamba, C. Curtis, Experimental hut trials of permethrin-impregnated mosquito nets and eave curtains against malaria vectors in Tanzania, Med. Vet. Entomol. 1 (1) (1987) 37–51.

[69] E.A. Mordecai, J.M. Cohen, M.V. Evans, P. Gudapati, L.R. Johnson, C.A. Lippi, K. Miazgowicz, C.C. Murdock, J.R. Rohr, S.J. Ryan, et al., Detecting the impact of temperature on transmission of Zika, dengue, and chikungunya using mechanistic models, PLoS Negl. Trop. Dis. 11 (4) (2017) e0005568.

[70] J.-F. Briere, P. Pracros, A.-Y. Le Roux, J.-S. Pierre, A novel rate model of temperature-dependent development for arthropods, Environ. Entomol. 28 (1) (1999) 22–29.

[71] M.F. Boyd, W.K. Stratman-Thomas, A note on the transmission of quartan malaria by anopheles Quadrimaculatus1, Am. J. Trop. Med. Hyg. 1 (3) (1933) 265–271.

[72] N. Bayoh, Studies on the development and survival of *Anopheles gambiae sensu stricto* at various temperatures and relative humidities, (Ph.D. thesis), University of Durham, UK, 2001.

[73] F.H. Johnson, S. Johnson, H. Eyring, B.J. Stover, The Theory of Rate Processes in Biology and Medicine, Wiley-Interscience, 1974.

[74] G. Englund, G. Öhlund, C.L. Hein, S. Diehl, Temperature dependence of the functional response, Ecol. Lett. 14 (9) (2011) 914–921.

[75] A.I. Dell, S. Pawar, V.M. Savage, Systematic variation in the temperature dependence of physiological and ecological traits, Proc. Natl. Acad. Sci. 108 (26) (2011) 10591–10596.
[76] F.J. Lardeux, R.H. Tejerina, V. Quispe, T.K. Chavez, A physiological time analysis of the duration of the gonotrophic cycle of A*nopheles pseudopunctipennis* and its implications for malaria transmission in Bolivia, Malar. J. 7 (1) (2008) 141.
[77] O. Diekmann, J. Heesterbeek, J.J. Metz, On the definition and the computation of the basic reproduction ratio R_0 in models for infectious diseases in heterogeneous populations, J. Math. Biol. 28 (4) (1990) 365–382.
[78] D.P.V. Den, W. J., Reproduction numbers and sub-threshold endemic equilibria for compartmental models of disease transmission, Math. Biosci. 80 (2002) 29.
[79] J. Dushoff, W. Huang, C. Castillo-Chavez, Backwards bifurcations and catastrophe in simple models of fatal diseases, J. Math. Biol. 36 (1998) 227–248.
[80] C. Castillo-Chavez, B. Song, Dynamical models of tuberculosis and their applications, Math. Biosci. Eng. 3 (2004) 361–404.
[81] A. Gumel, Causes of backward bifurcations in some epidemiological models, J. Math. Anal. Appl. 395 (1) (2012) 355–365.
[82] W. Wang, X.-Q. Zhao, Threshold dynamics for compartmental epidemic models in periodic environments, J. Dynam. Differential Equations 20 (3) (2008) 699–717.
[83] World Health Organization, et al., Guidelines for laboratory and field testing of long-lasting insecticidal mosquito nets, Technical Report, World Health Organization, 2005.
[84] World Health Organization, et al., Guidelines for laboratory and field-testing of long-lasting insecticidal nets, Technical Report, World Health Organization, 2013.
[85] S. Marino, I.B. Hogue, C.J. Ray, D.E. Kirschner, A methodology for performing global uncertainty and sensitivity analysis in systems biology, J. Theoret. Biol. 254 (1) (2008) 178–196.
[86] Z. Kambris, A.M. Blagborough, S.B. Pinto, M.S. Blagrove, H.C.J. Godfray, R.E. Sinden, S.P. Sinkins, Wolbachia stimulates immune gene expression and inhibits Plasmodium development in *Anopheles gambiae*, PLoS Pathogens 6 (10) (2010) e1001143.
[87] G.L. Hughes, R. Koga, P. Xue, T. Fukatsu, J.L. Rasgon, Wolbachia infections are virulent and inhibit the human malaria parasite *Plasmodium falciparum* in *Anopheles gambiae*, PLoS Pathogens 7 (5) (2011) e1002043.
[88] T. Walker, L.A. Moreira, Can wolbachia be used to control malaria? Memórias do Instituto Oswaldo Cruz 106 (2011) 212–217.